BUTTERWORTH HEINEMANN

Polymer Vol. 36 No. 20, pp. 3795–3801, 1995

0032-3861/95/$10.00+0.00

polymer papers

Morphology of syndiotactic polypropylene

Ralf Thomann, Chun Wang, Jörg Kressler*, Stephan Jüngling and Rolf Mülhaupt

Albert-Ludwigs-Universität Freiburg, Institut für Makromolekulare Chemie und Freiburger Materialforschungszentrum, Stefan-Meier-Strasse 31, D-79104 Freiburg/Breisgau, Germany

(Received 19 January 1995)

The morphology of syndiotactic polypropylene (s-PP), containing 91% racemic pentads, isothermally crystallized from the melt has been investigated by means of light microscopy, atomic force microscopy (AFM), and small-angle X-ray scattering (SAXS). Light microscopy shows a typical needle-like structure of crystalline entities at crystallization temperatures ranging from 115 to 150°C. Large bundles of lamellae and rectangular entities with single crystal character were the main morphological structures observed by AFM. These single crystal-like entities exhibit two typical fracture types; (i) transverse straight fractures with an average distance between the cracks of approximately 2 μm, and (ii) irregular fractures which yield a small mosaic-like structure. A lamellar thickness of 10 nm and a long period of 20 nm of s-PP crystallized isothermally at 135°C were obtained from the two-dimensional correlation function of SAXS measurements. This long period is in good agreement with that measured by AFM. Rare structures such as spherulites, hedrites and aggregates having a clear lateral periodicity perpendicular to the growth direction can be observed. Light microscopy of s-PP crystallized at 126°C and 3.5 kbar shows mainly spherulitic growth with an irregular banding structure.

(Keywords: syndiotactic polypropylene, atomic force microscopy, small-angle X-ray scattering)

INTRODUCTION

There is a growing interest in the structure and morphology of stereoregular polypropylenes. For isotactic polypropylene (i-PP), several extensive morphological studies have been published[1,2]. In contrast, studies about the morphology of syndiotactic polypropylene (s-PP) are still rare and were published only recently[3–6]. This delay is caused by the relatively late availability of highly syndioregular polypropylene, produced by using metallocene catalysts[7]. The dominant supermolecular appearance of s-PP published in the early 1980s was probably spherulitic because spherulite growth rates were measured[8]. This is in disagreement with recent publications and our observations and might be caused by the relatively poor stereoregularity of the s-PP used in ref. 8.

This investigation deals mainly with the observation of the morphology of highly syndioregular s-PP by means of light microscopy, atomic force microscopy (AFM) and small-angle X-ray scattering (SAXS). Because AFM is only able to detect polymer surfaces, the s-PP samples were etched with potassium permanganate dissolved in sulfuric acid.

EXPERIMENTAL

Sample preparation

The s-PP used in this study contains 91% racemic pentads, determined by ^{13}C-n.m.r. M_n is 104 000 g mol^{-1} determined by g.p.c. and M_w/M_a is 2.3. The catalyst system used for the synthesis of s-PP was $Me_2C(Cp)$-(Flu)$ZrCl_2$/MAO(Al/Zr = 2500). The polymerization was carried out in toluene at 20°C and 2 bar† propene pressure for 3 h. The catalyst concentration was 20 μmol l^{-1} and the activity was 1460 kg PP (mol bar h)$^{-1}$. The s-PP sample isothermally crystallized at 125°C has a melting point of 156°C measured by d.s.c. with a heat rate of 20°C min^{-1}.

Light microscopy

The samples for light microscopy were prepared by melting s-PP powder between two cover glasses. The layer thickness between these glasses was about 40 μm. The samples were held for 10 min at 180°C and then quenched to crystallization temperature at a rate of 30°C min^{-1}. The investigations were carried out with an Olympus-Vanox AH2 microscope and a Linkam TMS 90 hot stage that allows observation during isothermal crystallization. The light intensity was measured in the transmission mode with an equipped photo cell. The time dependence of the growth of crystalline entities was recorded with a video camera.

Etching procedure

The etching reagent was prepared by dissolving 0.02 g potassium permanganate in a mixture of 4 ml sulfuric acid (95–97%) and 10 g orthophosphoric acid. The acids were placed in a flask and stirred with a glass-covered magnetic stirrer; the potassium permanganate was

* To whom correspondence should be addressed
† 1 bar = 10^5 Pa

shaken into the swirling acids, the flask stoppered, and the mixture stirred until all the permanganate was dissolved. The 200 μm films of the s-PP were immersed in the freshly prepared etching reagent at room temperature and held there for 14 h; for the first 30 min the flask was held in an ultrasonic bath. For subsequent washings, a mixture of 2 parts by volume of concentrated sulfuric acid and 7 parts of water was prepared and cooled to near the freezing point with dry ice and isopropanol. The samples were washed successively with hydrogen peroxide (to reduce any manganese dioxide or permanganate present). Then the samples were washed with distilled water several times and finally with methanol. Each washing required about 15 min in an ultrasonic bath.

Atomic force microscopy (AFM)

The AFM experiments were carried out on a Nanoscope III scanning microscope (Digital Instruments Inc.) at ambient conditions. Measurements were performed with simultaneous registration of height and normal force (vertical cantilever deflection) images, which will be named HT and NF images, respectively. Si tips ('Nanoprobes') were employed with a force constant of about 0.1 N m^{-1}.

Small-angle X-ray scattering (SAXS)

The samples for SAXS measurement were isothermally crystallized at 135°C. The SAXS measurements were performed in an evacuated Kratky compact camera (Anton Paar K.G.) with an 80 μm entrance slit. Cu Kα radiation with a wavelength $\gamma = 0.154$ nm was used. The scattered intensity, I, was recorded by a scintillation counter in a step-scanning mode at room temperature. All scattering profiles were corrected for background scattering and desmeared[9]. Finally, the scattering caused by thermal density fluctuations was eliminated by computing the slope of an Is^4 *versus* s^4 plot at high scattering vectors, $s = (2/\gamma)\ \sin(\theta/2)$ where θ is the scattering angle[10].

High-pressure crystallization

The sample for high-pressure crystallization was made by melting s-PP powder between two cover glasses at 220°C. After reaching this temperature the pressure was raised to 3.5 kbar, then the sample was removed. This pretreatment is necessary in order to avoid shearing structures which occur in thicker samples without high pressure treatment. The isothermal and isobaric crystallization was carried out by remelting the pressed sample on a hot stage. The molten sample was immediately removed and placed into the preheated press and crystallized at 3.5 kbar and 126°C for 2 days.

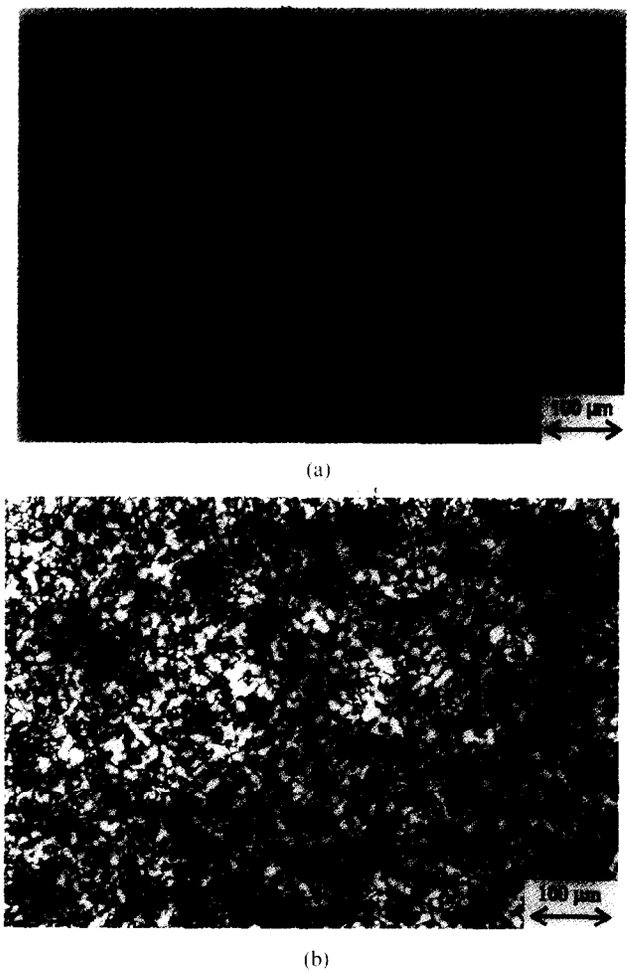

Figure 1 Light micrograph of s-PP crystallized at 137°C: (a) for 19 h where the polarizers are not completely crossed; (b) space-filling crystallized for 48 h between exactly crossed polarizers

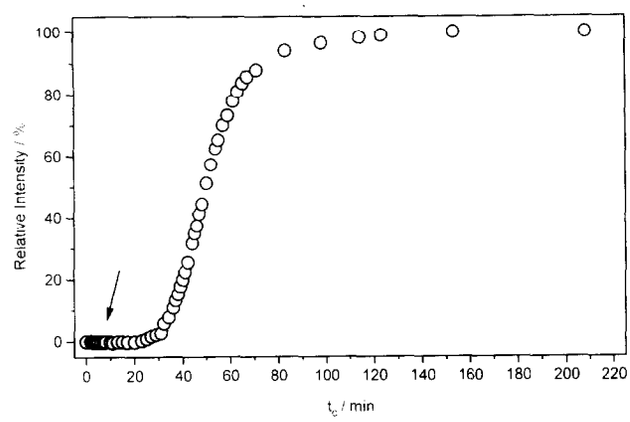

Figure 2 Relative light intensity between exactly crossed polarizers as a function of crystallization time at 125°C

RESULTS AND DISCUSSION

Microscopic observations

Figure 1a shows a light micrograph of s-PP crystallized at 137°C for 19 h, where polarizer and analyzer are not completely crossed. The typical appearance of needle-like entities can be seen. They can also be observed in the case of parallel polarizers, i.e. the needles have a different density from the melt. These needles are very typical over the whole temperature range of crystallization studied. *Figure 1b* shows the final morphology of s-PP crystallized at 137°C for 48 h under crossed polarizers. With exactly crossed polarizers the early stages of the s-PP crystallization can hardly be seen. This can be determined more quantitatively by measurements of the relative light intensity during the crystallization. *Figure 2* shows the relative light intensity between exactly crossed polarizers as a function of crystallization time at 125°C. An arrow indicates the time when the needle structures became visible with parallel polarizers. That the relative light intensity does not start to grow immediately after the

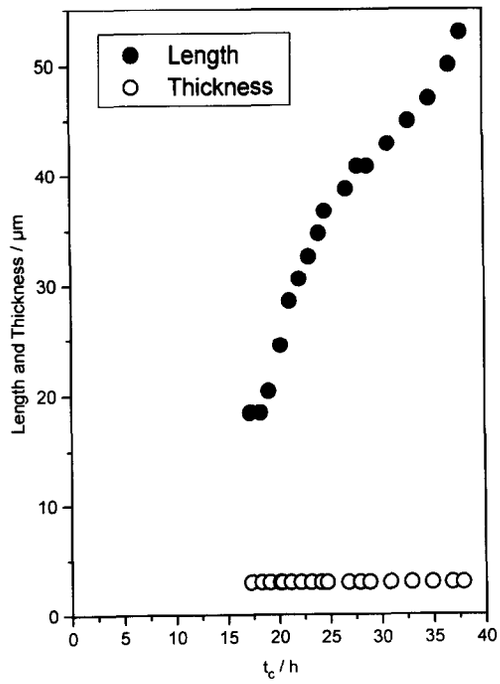

Figure 3 Length and thickness of needle-like entities of s-PP crystallized isothermally at 140°C as a function of time

needle-like structures appear might be for two reasons: first, that the initial stage of crystallization is very disordered (homogeneous nucleation), or second, that the lamellae are well ordered but the change of the plane of the polarized light is so small that it is not observable. This behaviour is significantly different from the crystallization of i-PP which in this temperature range shows exclusively spherulites. This leads already in the early stage to entities which are observable between crossed polarizers and simultaneously an increase of the relative light intensity is measured when the polarizers are crossed.

The growth of the s-PP needles is one-dimensional. *Figure 3* shows the length and thickness as a function of crystallization time of s-PP crystallized isothermally at 140°C, observed between incompletely crossed polarizers. The length is a nearly linear function of the time and the thickness does not change with time. The growth at lower crystallization temperatures cannot be measured, because the needles collide immediately after their appearance. Nevertheless the needle structure was also observed at all crystallization temperatures between 115 and 150°C.

The s-PP sample becomes bright between crossed polarizers in the late stage of crystallization (*Figures 1b* and *2*). A finely dispersed and apparently not well ordered structure can be seen. *Figure 4a* shows an AFM micrograph of a completely crystallized sample after permanganic etching. Typical bundles of lamellae (fibrils) show that space filling crystallization occurred. Furthermore, it can be seen that parallel-arranged fibrils occur over wide areas (indicated by arrows) which are assumed to belong to the original needles. Only after colliding might they bend and fringe. This leads to a densely packed structure. Schematically the development of this structure is depicted in *Figure 4b*. This appearance is also very different from AFM pictures of i-PP of the same scale. For i-PP the cross hatching can be clearly observed.

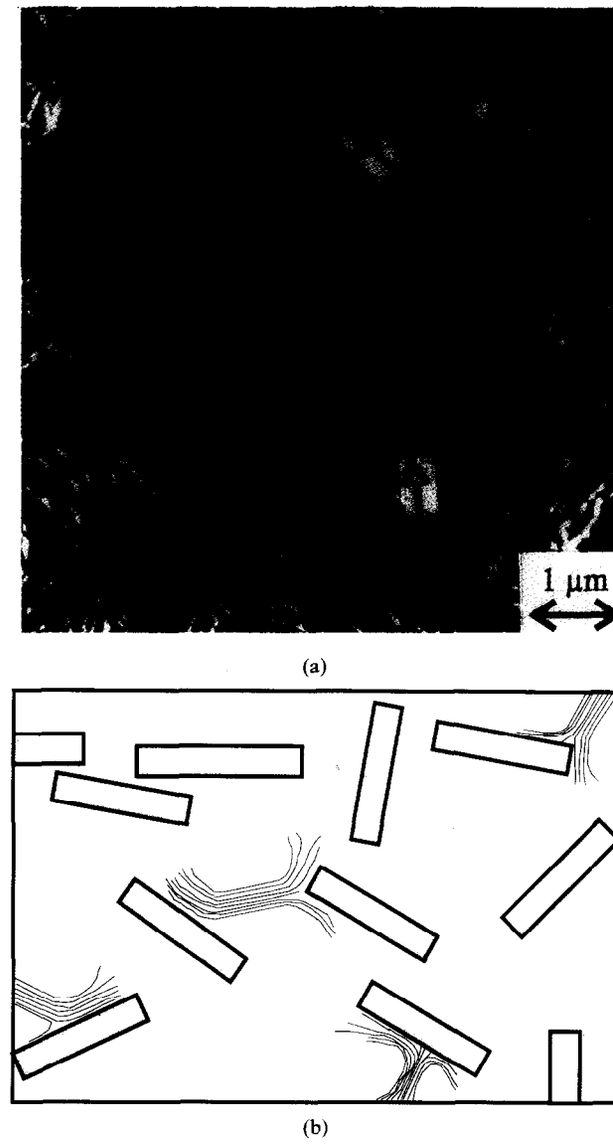

Figure 4 (a) AFM (NF) micrograph of a completely crystallized s-PP sample after permanganic etching (T_c = 135°C). (b) Scheme of the bending and fringing of lamellae bundles that lead to the structure depicted in (a)

Figure 5a shows a light micrograph of an s-PP sample between crossed polarizers crystallized at 147°C for 80 h. There are bundles of rodlike fibrils having only two growth directions with a common central point (nucleus). The same structure detected by AFM after permanganic etching can be seen in *Figure 5b*. It can clearly be observed that the fibrils grow straight, without bending and mainly without branching. This absence of branching seems to be the main reason that s-PP does not usually form spherulites.

Apart from these bundle structures, large s-PP multilayer, single crystal-like entities appear. AFM micrographs of these single crystal-like structures crystallized at 139°C for 19 h and quenched in liquid nitrogen are depicted in *Figures 6a* and *b*. Two different types of cracks in the single crystals, discussed already by Lovinger *et al.*[3], can be observed; transverse straight fractures with an average distance between the cracks of 2 µm (*Figure 6a*) and irregular fractures that yield a small mosaic-like structure (right part of *Figure 6b*). These mosaic-like parts were often etched away from their

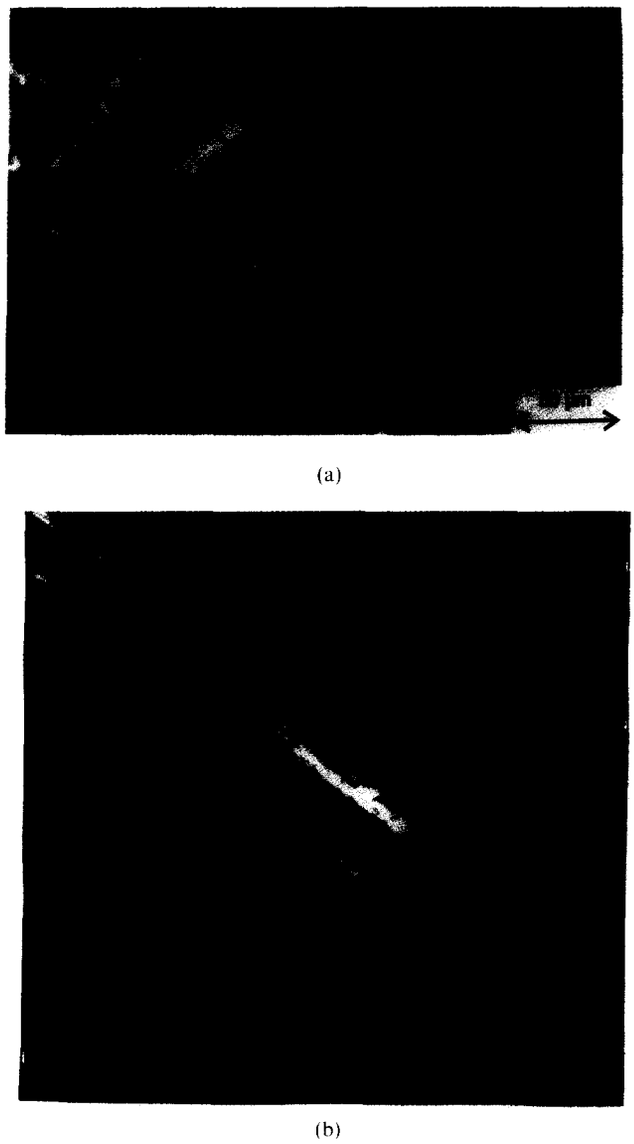

Figure 5 Bundles of rodlike lamellae. (a) Light micrograph of s-PP crystallized at 147°C for 80 h. (b) AFM (HT) micrograph of s-PP crystallized at 139°C for 19 h

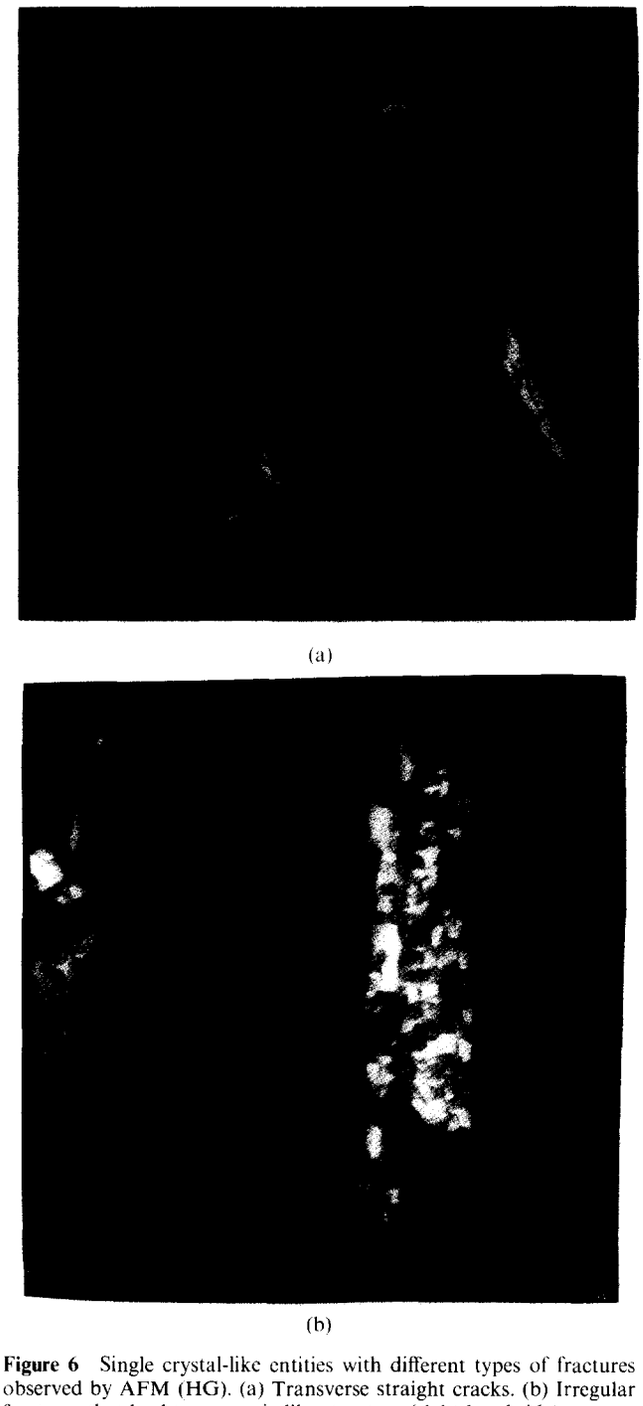

Figure 6 Single crystal-like entities with different types of fractures observed by AFM (HG). (a) Transverse straight cracks. (b) Irregular fractures that lead to a mosaic-like structure (right-hand side)

original growth alignment. Both fracture types might be caused by internal stresses beyond a critical value[3]. In the lower part of *Figure 6a* a crystal growth perpendicular to another crystal is observed. This might be caused by homoepitaxial growth, as described by Schumacher *et al.*[5].

These cracks can also be observed by light microscopy between crossed polarizers. *Figure 7a* depicts open, multi-faceted aggregates, and *Figure 7b* rodlike aggregates crystallized at 147°C having a clear lateral structure commonly perpendicular to the growth direction. In areas where these lateral structures can be detected, they have a distance of approximately 2 μm. Some of these areas are marked with an arrow in *Figure 7a*. This distance is in good agreement with the spacing of transverse cracks shown in *Figure 6a* and obtained by AFM measurements.

A close look at the single crystal-like entities described shows that they contain several layers packed parallel onto each other (*Figure 8*). The appearance of bright layers with dark spacings between them can only be explained by less ordered material confined between single crystals. This disordered material will be etched preferably and leads to dark (deeper) areas in the AFM images. These intercrystalline areas might contain amorphous material or also loops caused by chain folding. It can clearly be seen that the fractures run uniformly through the packed layers. Thus the fracture process is a cooperative event reflecting a connectivity of the single layers. The described structures, bundles of fibrils and fractured entities often appear together. *Figure 9* shows an AFM micrograph of an open aggregate with different types of crystallization morphologies. From a common centre bundles of fibrils and fractured entities start to grow.

Figure 10 depicts some rare structures occurring during the crystallization of s-PP at 145°C. In *Figure*

(a)

(b)

Figure 7 Light micrographs of s-PP crytallized at 147°C for 93 h and having a clear lateral structure. (a) Open, multi-faceted aggregates; (b) rodlike aggregates

Figure 8 Multiple layers of single crystal-like entities showing fracture structures observed by AFM (HT)

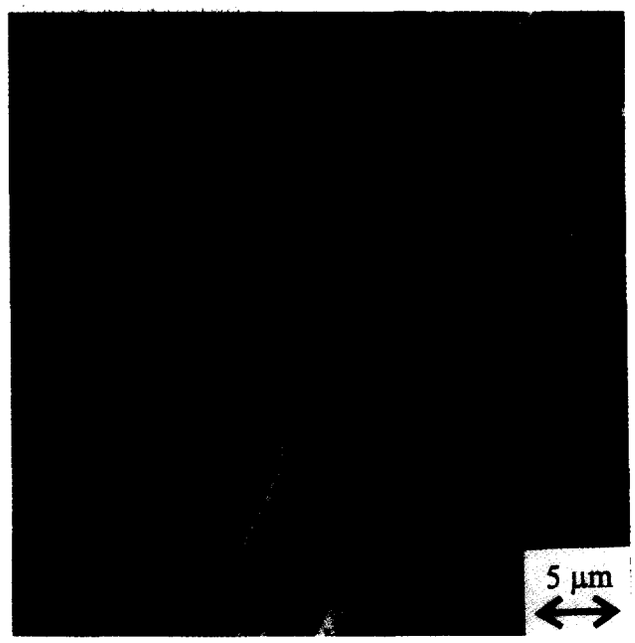

Figure 9 AFM (HT) micrograph of an open aggregate showing bundle structrues and single crystal-like entities

10a spherulites that are not regularly branched can be seen. It seems that they have one main growth direction (bright) and the branching in order to give a three-dimensional spherulite is hindered, i.e. the typical Maltese cross cannot be observed. *Figure 10b* represents spherulites with a star structure. This sample is space-filling crystallized. Lines of impingement of the spherulites are indicated by arrows. It can clearly be seen that completely dark areas also contribute to these lines. It must be mentioned that both spherulite types are different from the spherulites obtained by crystallizing a partially degraded s-PP. A sample annealed at 350°C for 15 min also shows after isothermal crystallization spherulites, probably caused by the degradation process, but these spherulites show a real Maltese cross. Furthermore, *Figure 10c* shows hedrites crystallized at 147°C. The existence of these hedrites is in agreement with the difficulty for s-PP to yield branched structures. Spherulites are rarely observed, but crystallized under high pressure they are the normal structure. *Figure 10d* shows spherulites, crystallized isothermally and isobarically at 126°C and 3.5 kbar. Like the spherulites in *Figure 10a*, these spherulites also do not show the common Maltese cross, but an irregular banding structure. Banded spherulites are usually caused by a cooperative bending process of lamallae[11,12].

The lamellar scale

SAXS has been used frequently to describe the lamellar thickness and the long period of semicrystalline polymers[13,14]. *Figure 11a* shows the desmeared and corrected SAXS trace for s-PP. Most characteristic is the maximum which belongs to the lamellar spacing. A higher order maximum occurs at $3s_{max}$. The second-order peak is obviously suppressed, i.e. the amorphous region between the lamellae have a similar thickness to the lamellae themselves. More quantitative information can be deduced from the Fourier transformation of the scattering curve, which yields the linear correlation

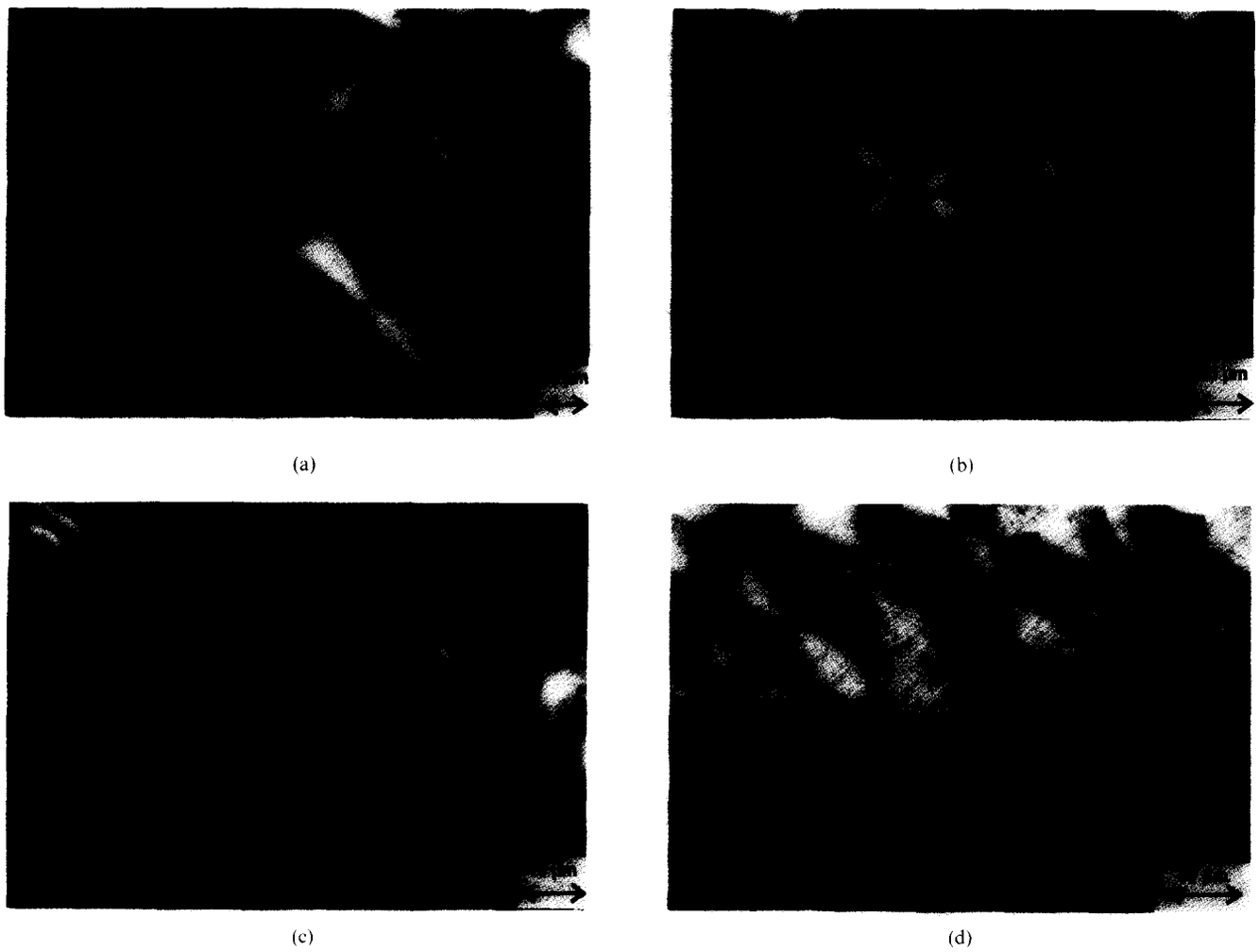

Figure 10 Light micrographs of rare structures. (a) Irregularly branched spherulites crytallized at 145°C for 134 h. (b) Spherulitic entities with a star structure crystallized at 145°C for 134 h. (c) Hedrites that occur in a sample crystallized at 147°C for 80 h. (d) Spherulites crystallized isothermally and isobarically at 126°C and 3.5 kbar

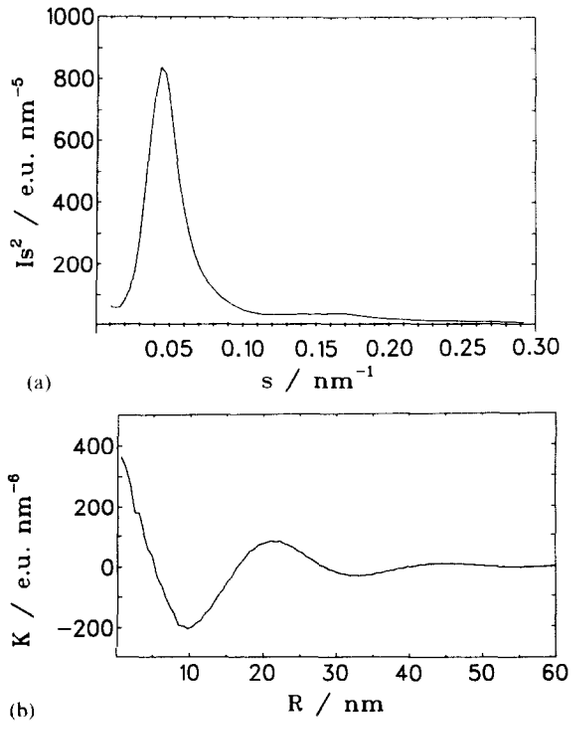

Figure 11 (a) Desmeared and corrected SAXS traces for s-PP crystallized at 135°C; (b) correlation function $K(z)$ for s-PP crystallized at 135°C

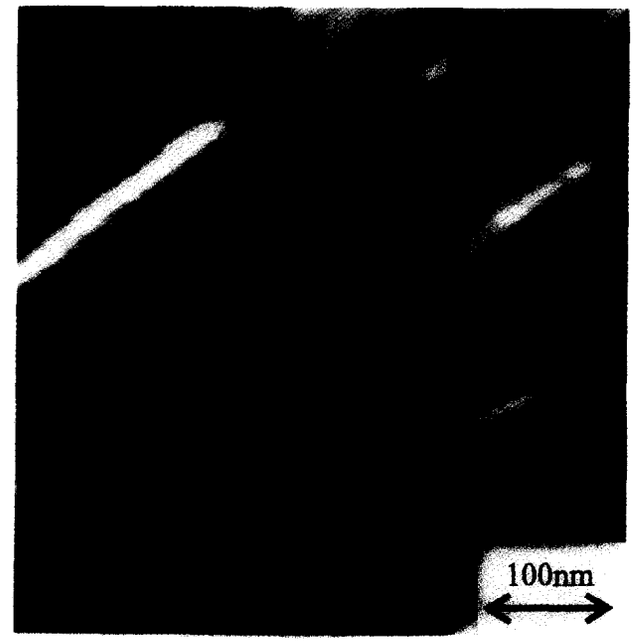

Figure 12 Magnified area of the AFM (NF) micrograph of *Figure 4a*; four edge-on lamellae are marked with a white bar perpendicular to these lamellae (length 62.5 nm)

function $K(z)$ defined by[15,16]

$$K(z) = \int_0^\infty 4\pi s^2 I(s) \cos^2 \pi sz \, ds$$

The correlation function for s-PP can be seen in *Figure 11b*. The position of the first minimum of the correlation function is related to the lamellar thickness, which is about 10 nm. The position of the first maximum of the correlation function can be assigned to the long period, i.e. the most probable next-neighbour distance of the lamellae. It can be seen that the long period is about 20 nm.

The long period could also be obtained from AFM. *Figure 12* shows a magnified part of *Figure 4a*. The small white bar perpendicular to four edge-on lamellae has a length of 62.5 nm. The average next-neighbour distance between the lamellae (long period) is about 20 nm. This is in good agreement with the values obtained by SAXS.

CONCLUSION

s-PP, crystallized from the melt, exhibits various types of structures, observable with light microscopy and with AFM. The most unusual property of s-PP is its incapacity to build up a three-dimensional structure, whereas in the case of isotactic PP spherulites are usually formed. s-PP is one of the rare polymers able to form large rectangular single crystal-like entities from the melt. They exhibit different fracture types, thus fragmented entities are usually formed. SAXS and AFM show that s-PP is well ordered after space-filling crystallization. Both methods give a lamellar thickness of 10 nm and a long period of about 20 nm for a sample isothermally crystallized at 135°C.

ACKNOWLEDGEMENTS

The authors thank BMFT for supporting this research as part of the BMFT project 03M40714. They thank the Bundesminister für Wirtschaft for supporting this work by the AIF-project 8529, and B. Heck and B. Stühn for carrying out SAXS measurements.

REFERENCES

1 Bassett, D. C. and Olley, R. H. *Polymer* 1982, **25**, 935
2 Norton, D. R. and Keller, A. *Polymer* 1985, **26**, 704
3 Lovinger, A. J., Lotz, B., Davis, D. D. and Schumacher, M. *Macromolecules* 1994, **27**, 6603
4 Stocker, W., Schumacher, M., Graff, S., Lang, J., Wittmann, J. C., Lovinger, A. J. and Lotz, B. *Macromolecules* 1994, **27**, 6948
5 Schumacher, M., Lovinger, A. J., Agarwal, P., Wittmann, J. C. and Lotz, B., *Macromolecules* 1994, **27**, 6956
6 Tsukruk, V. V. and Reneker, D. H., *Macromolecules* 1995, **28**, 1370
7 Ewen, J. A., Jones, R. L., Razavi, A. and Ferrara, J. D. *J. Am. Chem. Soc.* 1988, **110**, 6255
8 Miller, R. L. and Seeley, E. G. *J. Polym. Sci., Polym. Phys. Edn.* 1982, **20**, 2297
9 Strobl, G. R. *Acta Crystallogr.* 1970, **A26**, 367
10 Russell, T. P., Ito, H. and Wignall G. D. *Macromolecules* 1988, **21**, 1703
11 Keller, A. *Nature* 1952, **169**, 913
12 Keith, H. D. and Padden, F. J. *J. Appl. Phys.* 1963, **34**, 2409
13 Morrison, J. D., Burgess, A. N. and Stephensen, R. C. *Polymer* 1994, **35**, 2272
14 O'Kane, W. J., Young, R. J., Ryan, A. J., Bras, W., Derbyshire, G. E. and Maut, G. R. *Polymer* 1994, **35**, 1352
15 Strobl, G. R., Schneider, M. J. and Voigt-Martin, I. G. *J. Polym. Sci., Polym. Phys. Edn* 1980, **18**, 1361
16 Tanabe, Y., Strobl, G. R. and Fischer, E. W. *Polymer* 1986, **34**, 1147